Space Weather

RESEARCH ARTICLE
10.1029/2019SW002236

Counter-Electrojet Occurrence as Observed From C/NOFS Satellite and Ground-Based Magnetometer Data Over the African and American Sectors

John Bosco Habarulema[1,2], Gabrielle Lefebvre[3], Mark B. Moldwin[3], Zama T Katamzi-Joseph[1,2], and Endawoke Yizengaw[4]

[1]South African National Space Agency, Hermanus, South Africa, [2]Department of Physics and Electronics, Rhodes University, Grahamstown, South Africa, [3]Department of Climate and Space Sciences and Engineering, University of Michigan, Ann Arbor, MI, USA, [4]Space Science Application Laboratory, The Aerospace Corporation, El Segundo, CA, USA

Abstract An analysis of the counter-electrojet occurrence (CEJ) during 2008–2014 is presented for the African and American sectors based on local daytime (0700–1700 LT) observations from the Communications and Navigation Outage Forecasting System (C/NOFS) vertical ion plasma drift (equivalent to vertical $\mathbf{E} \times \mathbf{B}$ at an altitude of about 400 km) and ground-based magnetometers. Using quiet time ($Kp \leq 3$) data, differences and/or similarities between the two data sets with reference to local time and seasonal dependence are established. For the first time, it is shown that C/NOFS satellite data are consistent with magnetometer observations in identifying CEJ occurrences during all seasons. However, C/NOFS satellite data show higher CEJ occurrence rate for almost all seasons. With respect to local time, C/NOFS satellite observes more CEJ events than magnetometer observations by average of about 20% and 40% over the American and African sectors, respectively, despite both data sets showing similar trends in CEJ identification. Therefore, when a space weather event occurs, it is important to first establish the original variability nature and/or magnitude of the eastward electric field in equatorial regions before attributing the resulting changes to solar wind-magnetosphere and ionosphere coupling processes since CEJ events can be present even during quiet conditions.

Key Points:
- A statistical trend of CEJ events using C/NOFS satellite vertical ion plasma drift and magnetometer observations has been established
- Both C/NOFS satellite and magnetometer data show higher CEJ occurrence rate over the African sector than the American sector
- C/NOFS satellite data exhibit more CEJ events than magnetometer data by average of 20% (40%) over the American (African) sector

Correspondence to:
J. B. Habarulema,
jhabarulema@sansa.org.za

Citation:
Habarulema, J. B., Lefebvre, G., Moldwin, M. B., Katamzi-Joseph, Z. T., & Yizengaw, E. (2019). Counter-electrojet occurrence as observed from C/NOFS satellite and ground-based magnetometer data over the African and American sectors. *Space Weather*, *17*, 1090–1104. https://doi.org/10.1029/2019SW002236

Received 26 APR 2019
Accepted 1 JUL 2019
Accepted article online 5 JUL 2019
Published online 20 JUL 2019

1. Introduction

The equatorial electrojet (EEJ) is a natural phenomenon within the *E* region ionosphere and is a result of electric fields driven from neutral wind dynamics and geomagnetic field geometry at the equator. The EEJ is a strip of current that flows within about ±3° latitudes from the geomagnetic equator and is usually eastward during daytime. Sometimes, the direction of the current reverses to westward, a phenomenon called counter electrojet (CEJ) due to a number of physical mechanisms including (but not limited to) ionospheric variability during stratospheric warming periods (Siddiqui et al., 2018; Stening et al., 1996; Vineeth et al., 2009), westward prompt penetrating electric field leading to ionospheric disturbed dynamo (Kikuchi et al., 2000; Yizengaw et al., 2011), and vertical upward winds uplifting ions thereby cancelling the vertical polarization electric field (Raghavarao & Anandarao, 1980). Therefore, the complex variability of CEJ is influenced/modulated by variations in local time, longitude (mainly related to migrating and nonmigrating tides), seasonal dependence, lunar cycles, magnetic activity, and solar activity (Marriott et al., 1979; Mayaud, 1977; Rabiu et al., 2017; Rastogi, 1974b; Singh et al., 2018; Soares et al., 2018; Zhou et al., 2018). Since the CEJ's first detection (Gouin, 1962), various studies have investigated the CEJ occurrence based mainly on magnetometers deployed in equatorial and/or low-latitude regions (e.g., Alex & Mukherjee, 2001; Rastogi, 1974a, and references therein). With time, the emergence of Low Earth Orbit (LEO) satellites in conducting ionosphere-thermosphere investigations such as Magnetic Field Satellite, Republic of China Satellite, Challenging Minisatellite Payload (CHAMP), Communications and Navigation Outage Forecasting System (C/NOFS), and SWARM, LEO measurements became complementary data sources for EEJ or CEJ studies (e.g., Cohen & Achache, 1990; Fejer & Scherliess, 1998; Fejer et al., 2008; Kumar et al., 2016; Lühr et al., 2004; Rodrigues et al., 2015; Yizengaw & Groves, 2018; Zhou et al., 2018). CEJ studies can also be performed using Incoherent Scatter Radar over Jicamarca or the mode that operates to determine *E* region irregularities commonly known as the Jicamarca Unattended Long-Term Studies of Ionosphere and Atmosphere (JULIA) and

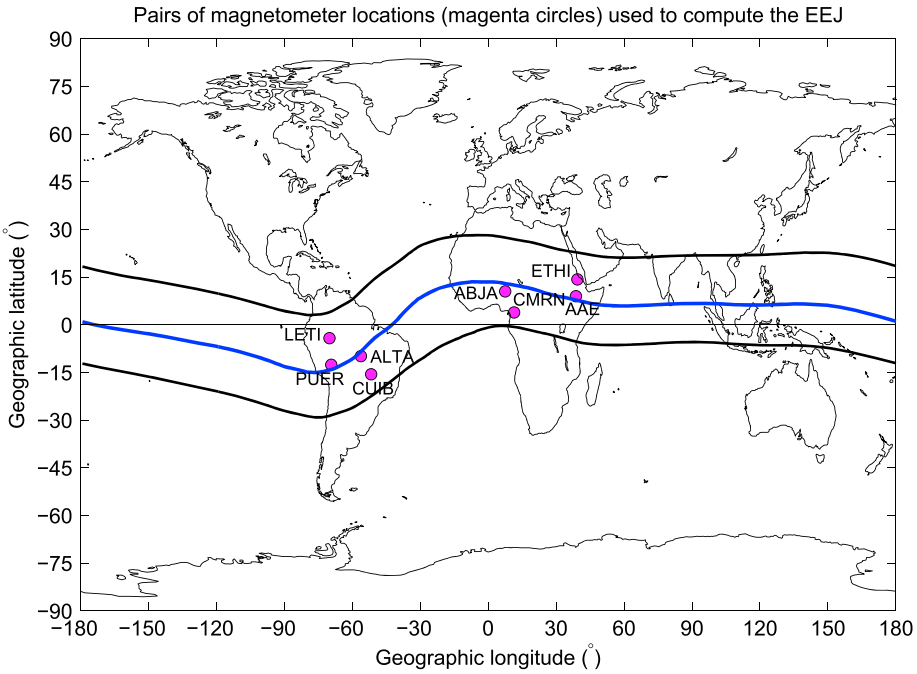

Figure 1. Pairs of magnetometer locations (magenta filled circles) used to compute EEJ in the African and American sectors. The blue line represents the geomagnetic equator. Black lines represent the crests of the equatorial ionization anomaly at ±15°. EEJ = equatorial electrojet.

similar coherent radar measurements in other longitude regions such as the Indian and Indonesian sectors (Patra et al., 2008, 2014). For example, Rodrigues et al. (2015) reported statistical results comparing C/NOFS Ion Velocity Meter (IVM) observations with 150-km echo drifts over the Peruvian sector during 2008–2009. While different sources of vertical drifts' measurements exist, it still remains a challenge to understand ionospheric dynamics and electrodynamics in some longitude regions with very limited information such as the African region and over the oceanic areas. In the context of radar and satellite measurements, the latter is attractive owing to the satellite's ability to sample all longitude sectors, providing measurements on global scales. The shortcoming of satellite measurements is the inability to provide continuous temporal variability of vertical drift data over a certain longitude sector, thus only providing "snapshots," making its data applicable for long-term climatology studies. In the absence of "expensive" radar infrastructure, other ground-based instrumentation such as magnetometers provide EEJ/CEJ information and hence vertical plasma drifts (e.g., Anderson et al., 2002, 2004; Habarulema et al., 2018; Yizengaw et al., 2014), although this is mainly limited to local daytime. This paper is aimed at statistically comparing the CEJ occurrences identified from ground-based magnetometer and C/NOFS observations over the American and African sectors during 2008–2014. The motivations for performing this fairly detailed analysis are based on earlier studies which showed that ground-based and satellite observations sometimes do not agree in identifying the downward drifts during similar local times (e.g., Rodrigues et al., 2015) and to establish the extent of agreement/disagreement based on local time. One of the implications of this study lies in the correct interpretation of results from models developed by combining both ground- and satellite-based observations to describe the equatorial electrodynamics. For event(s) analyses, variations in EEJ/CEJ provide insights into the variability of the equatorial ionization anomaly during geomagnetically disturbed conditions (Stolle et al., 2008; Venkatesh et al., 2015) and are thus an important parameter to accurately describe in order to understand the evolution and/or drivers of space weather events. Therefore, when a space weather event occurs, it is important to first establish the original variability nature and/or magnitude of the eastward electric field in equatorial regions before attributing the resulting changes to solar wind-magnetosphere and ionosphere coupling processes since CEJ events can be present even during quiet conditions.

Table 1
Geographic and Geomagnetic Coordinates of Magnetometer Stations Used to Estimate EEJ Over the American and African Sectors in This Study

Location/country	Code	Source	Geographic coordinates		Geomagnetic coordinates	
			Latitude	Longitude	Latitude	Longitude
		African sector				
Abuja (Nigeria)	ABJA	AMBER	10.5	7.6	−0.6	79.6
Yaounde (Cameroon)	CMRN	AMBER	3.9	11.5	−5.3	83.1
Addis Ababa (Ethiopia)	AAE	INTERMAGNET	9.0	38.8	0.2	110.5
Adigrat (Ethiopia)	ETHI	AMBER	14.3	39.5	6.0	111.1
		American sector				
Puerto Maldonado (Peru)	PUER	LISN	−12.6	−69.2	0.0	2.0
Leticia (Brazil)	LETI	LISN	−4.2	−69.9	8.2	2.0
Alta Floresta (Brazil)	ALTA	LISN	−9.9	−56.1	0.8	15.2
Cuiaba (Brazil)	CUIB	LISN	−15.6	−56.1	−5.9	13.8

Note. EEJ = equatorial electrojet; AMBER = African Meridian and *B*-Field Education Research; INTERMAGNET = International Real-time Magnetic Observatory Network; LISN = Low Latitude Ionospheric Sensor Network.

2. C/NOFS and Magnetometer Data Treatment

Satellite and magnetometer data were analyzed during geomagnetically quiet conditions based on the planetary *Kp* ($Kp \leq 3$) index criterion. The *Kp* index data were downloaded from wdc.kugi.kyoto-u.ac.jp/kp/index.html. The in situ equivalent vertical $\mathbf{E} \times \mathbf{B}$ drift data are estimated from the IVM drift measurements on board C/NOFS satellite, averaged within the altitude range of 400–550 km (Stoneback et al., 2011, 2012; Rodrigues et al., 2015; Yizengaw et al., 2014) during 2008–2014. Due to the intention of directly comparing with magnetometer-derived EEJ, it was necessary to limit the latitudinal coverage of satellite's data around the geomagnetic equator by constraining the latitude of observations to remain within the EEJ band. For this purpose, the latitude range used was ±4° around the geomagnetic equator and within a longitude range of ±8° centered around the meridian of the pair of magnetometer stations (e.g., Dubazane & Habarulema, 2018; Habarulema et al., 2018) for both African and American sectors. In an effort to minimize potential outliers associated with C/NOFS vertical ion plasma drift data within 400–550 km, we employed the median and scaled median absolute deviation (e.g., Huber, 1981; Huber & Ronchetti, 2009) for each satellite track during the entire period (2008–2014) of analysis. This filtering method has been previously used in related analyses (e.g., Dubazane & Habarulema, 2018; Habarulema et al., 2018; Lomidze et al., 2017) and is demonstrated in Dubazane and Habarulema (2018) for C/NOFS satellite data treatment. After removing outliers, the C/NOFS data are averaged in 3-min intervals. For the EEJ/CEJ measurements, we used two pairs of ground-based magnetometers in both African and American sectors during the period of 2008–2014. Figure 1 shows the locations of magnetometers that we used for this study. The geographic and geomagnetic coordinates are shown in Table 1 along with the exact locations and country. The corrected geomagnetic coordinates (Gustafsson et al., 1992) are obtained from geographic coordinates based on the International Geomagnetic Reference Field model for the Epoch year 2010. In the African sector, apart from AAE which is part of the INTERMAGNET (International Real-time Magnetic Observatory Network), the rest of the magnetometer stations are operated under the auspice of the AMBER (African Meridian and B-Field Education Research) project (Yizengaw & Moldwin, 2009; Yizengaw et al., 2011). The two pairs of magnetometer locations used in Africa are Addis Ababa (AAE; 9.0°N, 38.8°E) and Adigrat (ETHI; 14.3°N, 39.5°E) for the east African sector, and Abuja (ABJA; 10.5°N, 7.6°E) and Yaounde (CMRN; 3.9°N, 11.5°E) for west African sector. All South American magnetometer stations in Table 1 form part of the LISN (Low Latitude Ionospheric Sensor Network) project (Valladares & Chau, 2012). These are Puerto Maldonado (PUER; 12.6°S, 69.2°W) and Leticia (LETI; 4.2°S, 69.9°W), and Alta Floresta (ALTA; 9.9°S, 56.1°W) and Cuiaba (CUIB; 15.6°S, 56.1°W). Magnetometer data used in this study are freely available from http://magnetometers.bc.edu/, www.intermagnet.org, and http://lisn.igp.gob.pe/data/ for AMBER, INTERMAGNET, and LISN networks, respectively.

Each pair of magnetometer locations was used to compute the EEJ from the Earth's geomagnetic field's horizontal component following the established standard procedure done in many sources (e.g.,

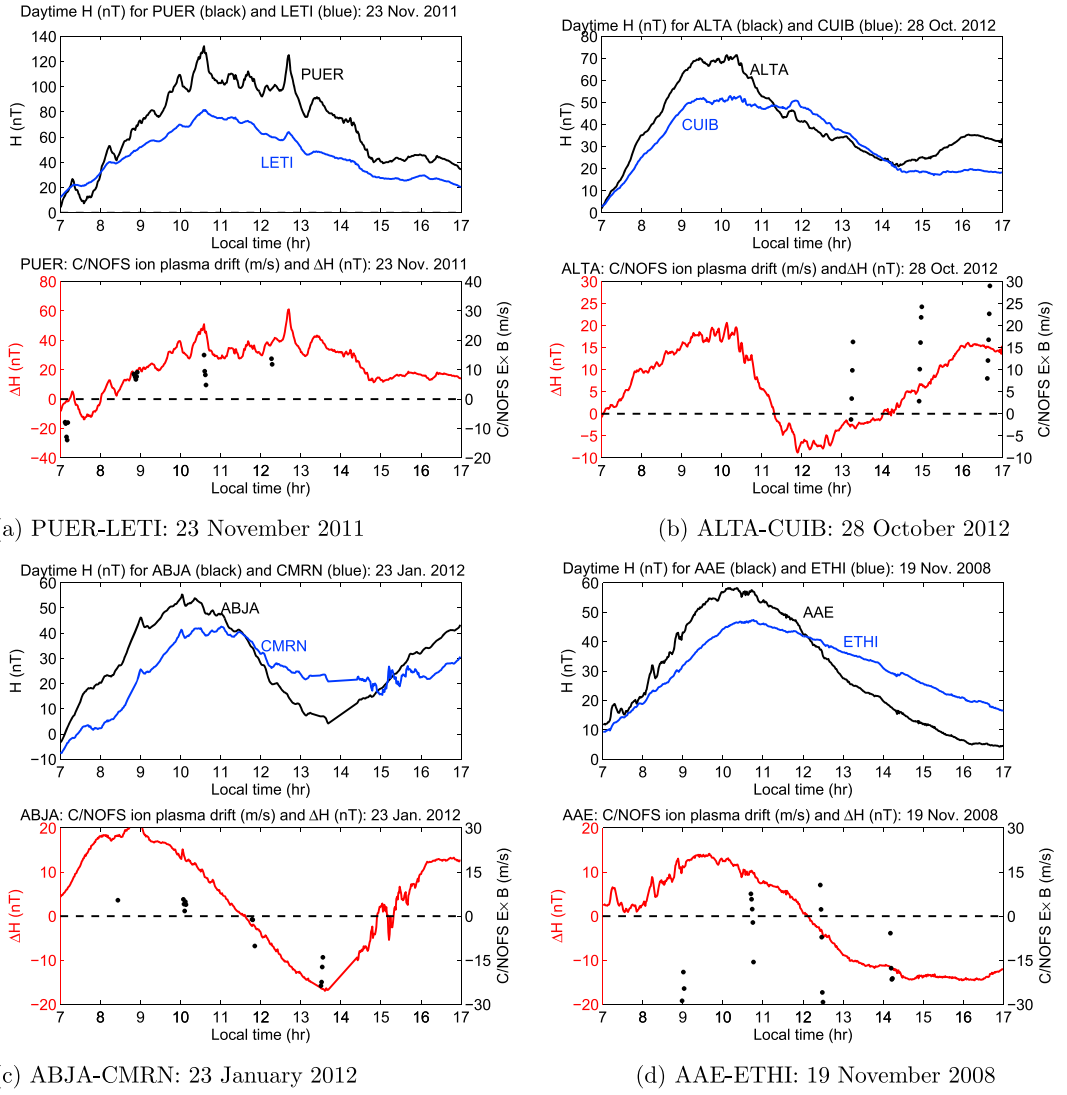

(a) PUER-LETI: 23 November 2011

(b) ALTA-CUIB: 28 October 2012

(c) ABJA-CMRN: 23 January 2012

(d) AAE-ETHI: 19 November 2008

Figure 2. Examples of horizontal component of the geomagnetic field with derived equatorial electrojet changes and available C/NOFS vertical ion plasma drift (**E** × **B** drift, plotted as black dots) for longitude sectors of (a) 69°W (23 November 2011), (b) 56°W (28 October 2012), (c) 9°E (23 January 2012), and (d) 39°E (19 November 2008), respectively. C/NOFS = Communications and Navigation Outage Forecasting System.

Anderson et al., 2002, 2004; Yizengaw et al., 2012). This procedure is based on differencing the horizontal component measurements (after removing the average nightime baseline value) of a magnetometer displaced by 6–9° from the geomagnetic equator from the corresponding *H* values measured by the magnetometer at the equator. The estimated EEJ is a proxy of low latitude vertical **E** × **B** drift (e.g., Anderson et al., 2004; Habarulema et al., 2018; Yizengaw et al., 2011). Figure 2 shows local daytime changes in *H* component after removing the nightside (2300–0300 local time) baseline measured at the equator and off the equator and the differences between the two representing the EEJ for randomly selected days over the American (PUER-LETI [23 November 2011] and ALTA-CUIB [28 October 2012]) and African (ABJA-CMRN [23 January 2012] and AAE-ETHI [19 November 2008]) regions. Superimposed on the Δ*H* (nT) plots are the available vertical ion plasma drift values from C/NOFS satellite (simply represented as vertical **E** × **B** drift indicated as black dots).

In Figure 2, there are periods when both C/NOFS satellite and Δ*H* (nT) data agree in identifying either upward or downward vertical drifts. Noticeable differences are also visible as in the case for Figure 2b (bottom panel), where Δ*H* (nT) was mostly negative between 1300 and 1400 LT (corresponding to downward vertical drifts) while C/NOFS observations show upward drifts or vice versa (see Figure 2d between 0900

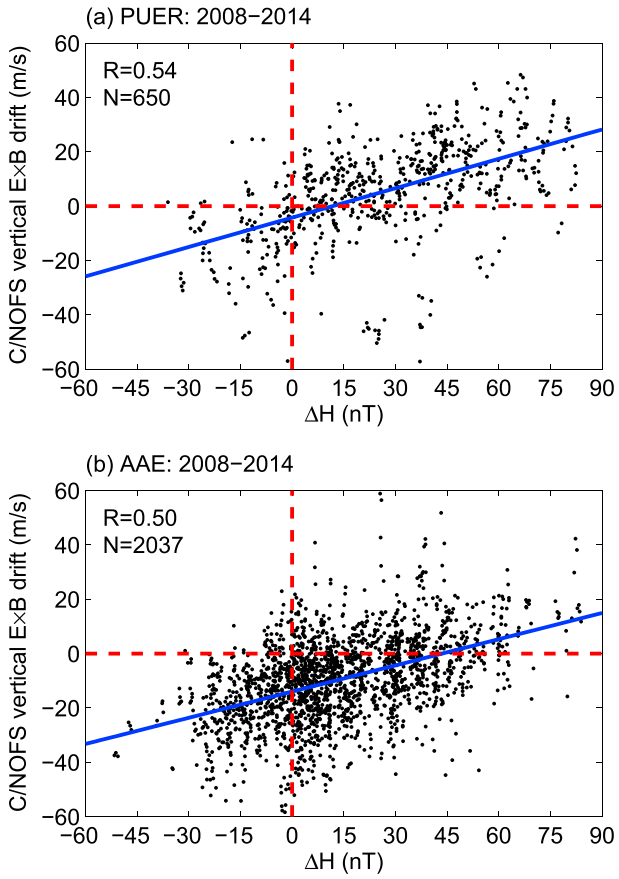

Figure 3. Scatter plot of C/NOFS vertical $\mathbf{E} \times \mathbf{B}$ drift against ΔH over PUER (a; American sector) and AAE (b; African sector) from 2008 to 2014. In (a) and (b), N represents the total number of data points. C/NOFS = Communications and Navigation Outage Forecasting System.

and 1100 LT for AAE on 19 November 2008). This highlights one of the reasons why we have decided to statistically study the differences and similarities between these data sets in showing CEJ occurrences.

3. Results and Discussion

Due to the unusual extended solar minimum at the end of solar cycle 23 during 2008–2010 (e.g., Chen et al., 2011; Ezquer et al., 2014) when vertical $\mathbf{E} \times \mathbf{B}$ drift did not show expected direct relationship with solar activity (e.g., Dubazane & Habarulema, 2018; Habarulema et al., 2018), the presentation of results is categorized into two periods of 2008–2010 and 2011–2014, respectively, for both the American and African sectors. This was however done only for the 69°W (American) and 38°E (African) longitude sectors where 2008–2014 data were available; otherwise, 2011–2014 data sets were analyzed for the 56°W (American) and 9°E (African) longitude sectors. A recent detailed investigation about CEJ occurrence with respect to different variables including solar activity using average properties derived from CHAMP data during 2000–2010 reported more occurrence rates for low solar flux levels (Zhou et al., 2018). For direct comparisons, magnetometer-derived ΔH was only considered at epochs when C/NOFS data were available; otherwise magnetometer data are extensively available. There were however few instances where C/NOFS data were available with no corresponding magnetometer data and these cases were also not included in the analysis. To identify CEJ occurrence, we have simply considered cases where C/NOFS vertical $\mathbf{E} \times \mathbf{B}$ drift and ΔH are negative (less than 0); thus, we do not have any threshold magnitude for each of these parameters. Figure 3 shows scatter plots of C/NOFS vertical $\mathbf{E} \times \mathbf{B}$ drift against ΔH for PUER and AAE representing American and African sectors, respectively. For the entire data sets, correlation values of 0.54 and 0.50 were obtained between C/NOFS vertical $\mathbf{E} \times \mathbf{B}$ drift and ΔH for PUER and AAE, respectively. The derived ΔH data from PUER-LETI pair of magnetometer stations is mostly available from 2009 and further contains significant data gaps especially in 2010–2011, explaining the difference in data points displayed in scatter plots of Figure 3 for PUER

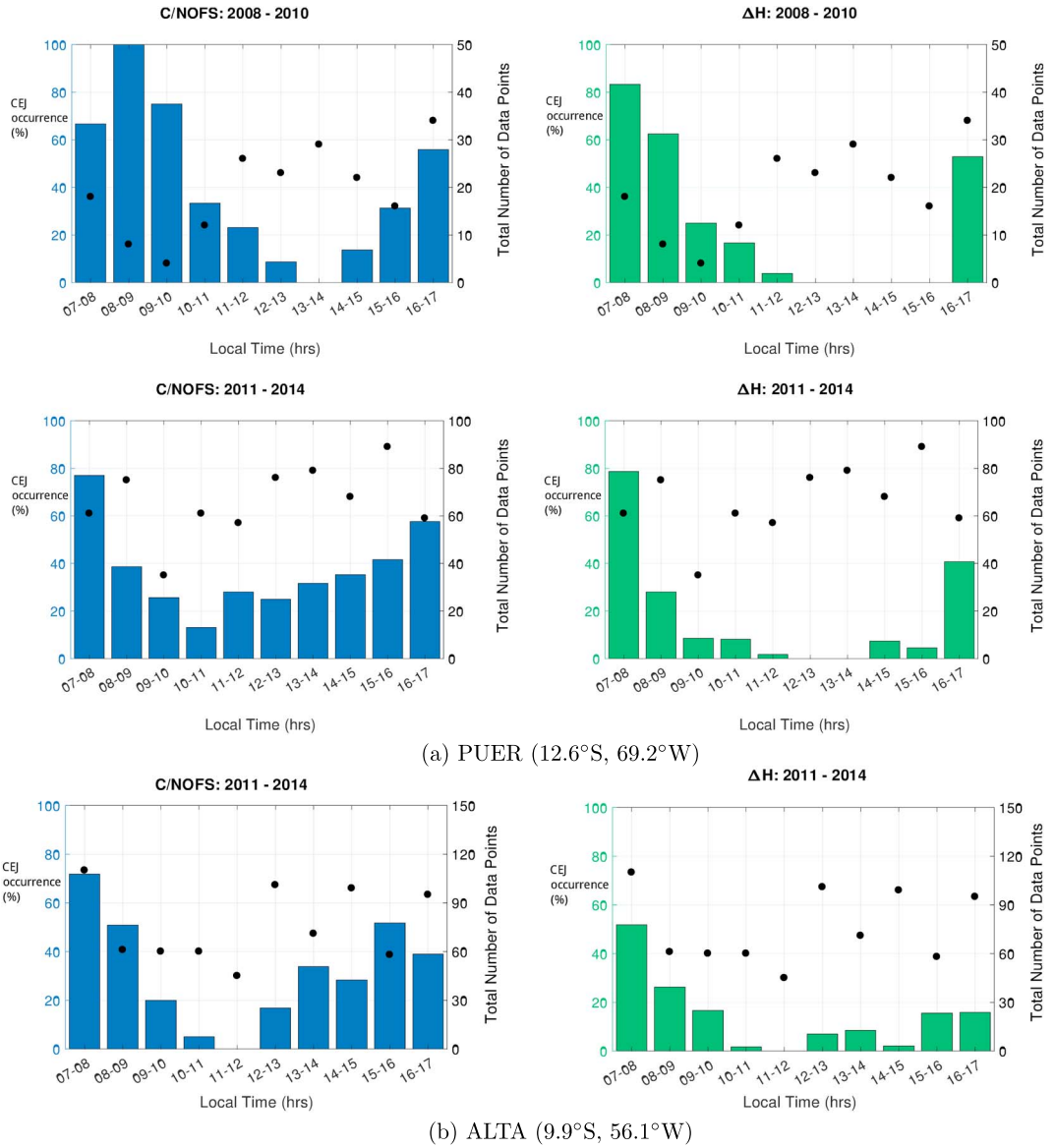

(a) PUER (12.6°S, 69.2°W)

(b) ALTA (9.9°S, 56.1°W)

Figure 4. Local time observations of CEJ occurrences as observed from C/NOFS satellite and ground-based magnetometer data, separately during 2008–2010 and 2011–2014 over (a) PUER (12.6°S, 69.2°W) and (b) ALTA (9.9°S, 56.1°W), within the American sector. CEJ = counter electrojet; C/NOFS = Communications and Navigation Outage Forecasting System.

and AAE. The correlation values are comparable to earlier results which reported values of 0.57 and 0.51 over Jicamarca (Habarulema et al., 2018) and AAE (Dubazane & Habarulema, 2018), respectively, between C/NOFS vertical $\mathbf{E} \times \mathbf{B}$ drift and ΔH. The low correlation values are attributed to the altitude differences at which C/NOFS vertical $\mathbf{E} \times \mathbf{B}$ drift and ΔH are computed. ΔH represents EEJ which is typically in the E region (about 110 km), while C/NOFS vertical ion plasma drift (equivalent to vertical $\mathbf{E} \times \mathbf{B}$ drift at 400 km) was estimated within an altitude range of 400–550 km. Furthermore, the variation of neutral wind velocity with respect to altitude in low latitudes can alter "the ground magnetic perturbation a few degrees" off the magnetic equator (Fambitakoye et al., 1976; Fang et al., 2008) and therefore contribute to the differences between derived ΔH and C/NOFS vertical $\mathbf{E} \times \mathbf{B}$ drift observations. Figure 3 shows that the C/NOFS satellite and ΔH observed more CEJ occurrence over the African sector (AAE) compared to the American sector (PUER). Statistically, negative $\mathbf{E} \times \mathbf{B}$ drift (ΔH) values interpreted as CEJ events account for 36%(18%) for PUER (Figure 3a) and 75% (28%) over AAE (Figure 3b). With regard to C/NOFS satellite data, our results are in agreement with previous seasonal analysis based on IVM data from 2009/2010 to 2013 that showed

vertical $\mathbf{E} \times \mathbf{B}$ drift values in the African sector to be dominated by negative values (with a slight exception for September equinox) compared to the American sector (Yizengaw et al., 2014; Yizengaw & Groves, 2018). In Figure 3b, an attempt to derive a direct relationship between the two parameters shows that a significantly large value of positive ΔH is required for an upward vertical drift at C/NOFS satellite altitude in the African sector. In both sectors, C/NOFS satellite observes more downward drifts than the magnetometer method, although a higher occurrence rate is more pronounced in the African sector. Being at a low inclination (13°) angle within an elliptical orbit, the C/NOFS satellite provides relatively detailed information within low/equatorial latitudes at all longitude sectors than other LEO satellites such as the ones in near polar orbit.

3.1. Local Time Occurrence of CEJ Over the American Sector

We have analyzed CEJ occurrences by looking at the number of times when the C/NOFS vertical $\mathbf{E} \times \mathbf{B}$ drift and ΔH were negative within hourly bins (07–08 LT, 08–09 LT, … , 16–17 LT) during magnetically quiet conditions ($Kp \leq 3$). Figure 4 shows diurnal CEJ occurrences (expressed as a percentage of total number of data points within an hour) as observed by C/NOFS and magnetometer-derived ΔH data over (a) PUER (12.6°S, 69.2°W) and (b) ALTA (9.9°S, 56.1°W) within the American sector. C/NOFS and ΔH CEJ identification results are plotted in blue and green bars, respectively. In both cases, the right-hand side of each subplot indicates the total number of data points (plotted as black dots) when coincidental observations were obtained simultaneously from C/NOFS and ΔH measurements. ALTA had magnetometer data for simultaneous analyses with C/NOFS data during 2011–2014. Otherwise, results over PUER (a) correspond to CEJ occurrence as detected by C/NOFS and ΔH observations for the periods of 2008–2010 and 2011–2014, respectively. In general, both C/NOFS and magnetometer data show that CEJ usually occurs during morning and evening times, a result similar to previous findings over the African and American sectors based on 2009 magnetometer data (Rabiu et al., 2017). The main difference from Figure 4 is that C/NOFS data show more cases in CEJ occurrences than magnetometer data in the afternoon hours for both PUER and ALTA. While this is mostly evident, a specific example in Figure 4b is for the case of 1500–1600 LT where CEJ occurrence identified by C/NOFS data is more than double the corresponding result for magnetometer observations. Using radar and C/NOFS data sets during 2008–2009 over Jicamarca, Rodrigues et al. (2015) observed that the C/NOFS afternoon downward vertical drift values did not feature in the 150-km echoes, which by inference may be true for ΔH as both JULIA and ΔH observations are all approximately within the E region (e.g., Anderson et al., 2004). In particular, we note that the percentage CEJ occurrences from magnetometer-derived ΔH is either less than 20% or absent during local times 1000–1600 LT for both 2008–2010 and 2011–2014. In fact, this observation can be extended to start from 0900 LT, with the exception of PUER results during 2008–2010. While the same consistency is not visible for C/NOFS observations, CEJ identification occurrences which are less than 20% can be noticed during 1200–1500 LT (2008–2010) and 1000–1300 LT (2011–2014) over PUER and ALTA, respectively. Based on the criteria defined in Alex and Mukherjee (2001) while analyzing magnetometer data over the African and Indian sectors, Chandrasekhar et al. (2017) reported high CEJ occurrence rate during morning hours (0700–1000 LT) followed by evening (1500–1800 LT), afternoon (1200–1500 LT), and lastly noon hours (1000–1200 LT). This is well reflected in Figure 4 for both PUER and ALTA (longitude separation of 13°) for C/NOFS and magnetometer data, although the percentage CEJ occurrence rate may be different in some cases. Zhou et al. (2018) showed that CEJ occurence rate reduces to about 4% at noon. Differences in CEJ occurrence rate between SWARM satellite and magnetometer observations have been recently reported (Soares et al., 2018), but their "qualitative agreement" was emphasized. Morning CEJ occurrence in ΔH is therefore dominant for both PUER (69.2°W longitude) and ALTA (56.1°W longitude). For the Brazilian sector where ALTA lies, our results are consistent with findings in Venkatesh et al. (2015) and Soares et al. (2018). Statistically, C/NOFS data are in agreement with magnetometer observations in showing predominantly morning CEJ occurrence with about 80% and 48% for PUER during 2008–2010 and 2011–2014, respectively, and 50% for ALTA in 2011–2014 during 0700–1000 LT. The rest of the CEJ occurrence rate is spread over other local times, but with afternoon CEJ occurrence being more predominant from C/NOFS observations. The presence of afternoon downward vertical drifts in C/NOFS vertical ion plasma drift data when the 150-km echo drifts from the JULIA experiment showed largely upward drifts over Jicamarca has been reported (Rodrigues et al., 2015). Due to the altitude of the C/NOFS satellite, these afternoon downward drifts (CEJ in this case) were attributed to the possibility of increased magnitude of semidiurnal tides in the topside ionosphere (Stoneback et al., 2011; Rodrigues et al., 2015). With respect to local time, this quiet time analysis shows that C/NOFS satellite observes more CEJ events than

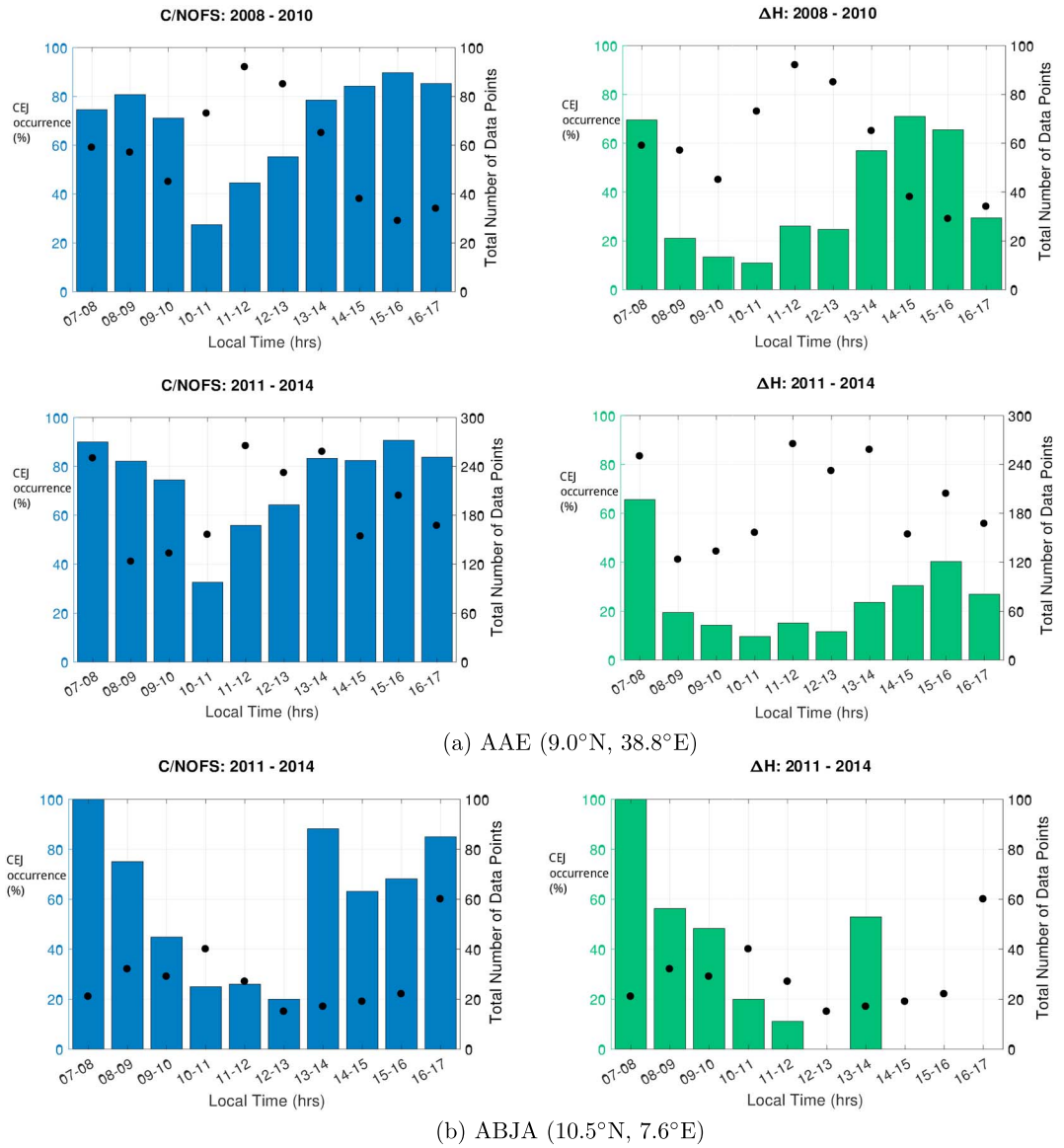

Figure 5. Local time observations of CEJ occurrences as observed from C/NOFS satellite and ground-based magnetometer data, separately during 2008–2010 and 2011–2014 over (a) AAE (9.0°N, 38.8°E) and (b) ABJA (10.5°N, 7.6°E), within the African sector. CEJ = counter electrojet; C/NOFS = Communications and Navigation Outage Forecasting System.

magnetometer observations by average of about 20% over the American sector, despite both data sets showing similar trends in CEJ identification. The result of the same trend from C/NOFS data at all local times with magnetometer data is important as satellite data augment the modelling approaches of vertical $\mathbf{E} \times \mathbf{B}$ drift on both regional and global scales. Regarding the existence of CEJs during different geomagnetic conditions, Zhou et al. (2018) showed that the CEJ occurrence rate increases with increase in geomagnetic activity. Nevertheless, there is significant CEJ occurrence during quiet conditions, and therefore, when a space weather event occurs, detailed investigation should be done to first understand the behavior of the eastward electric field in low/equatorial latitudes before concluding about the effects of disturbed dynamo electric fields. This has the potential to assist in future development of improved vertical $\mathbf{E} \times \mathbf{B}$ drift models for accurate specification of space weather effects and their variability on the ionosphere. A brief summary of suggested mechanisms (and relevant literature references) responsible for occurrence of CEJ is presented in Zhou et al. (2018).

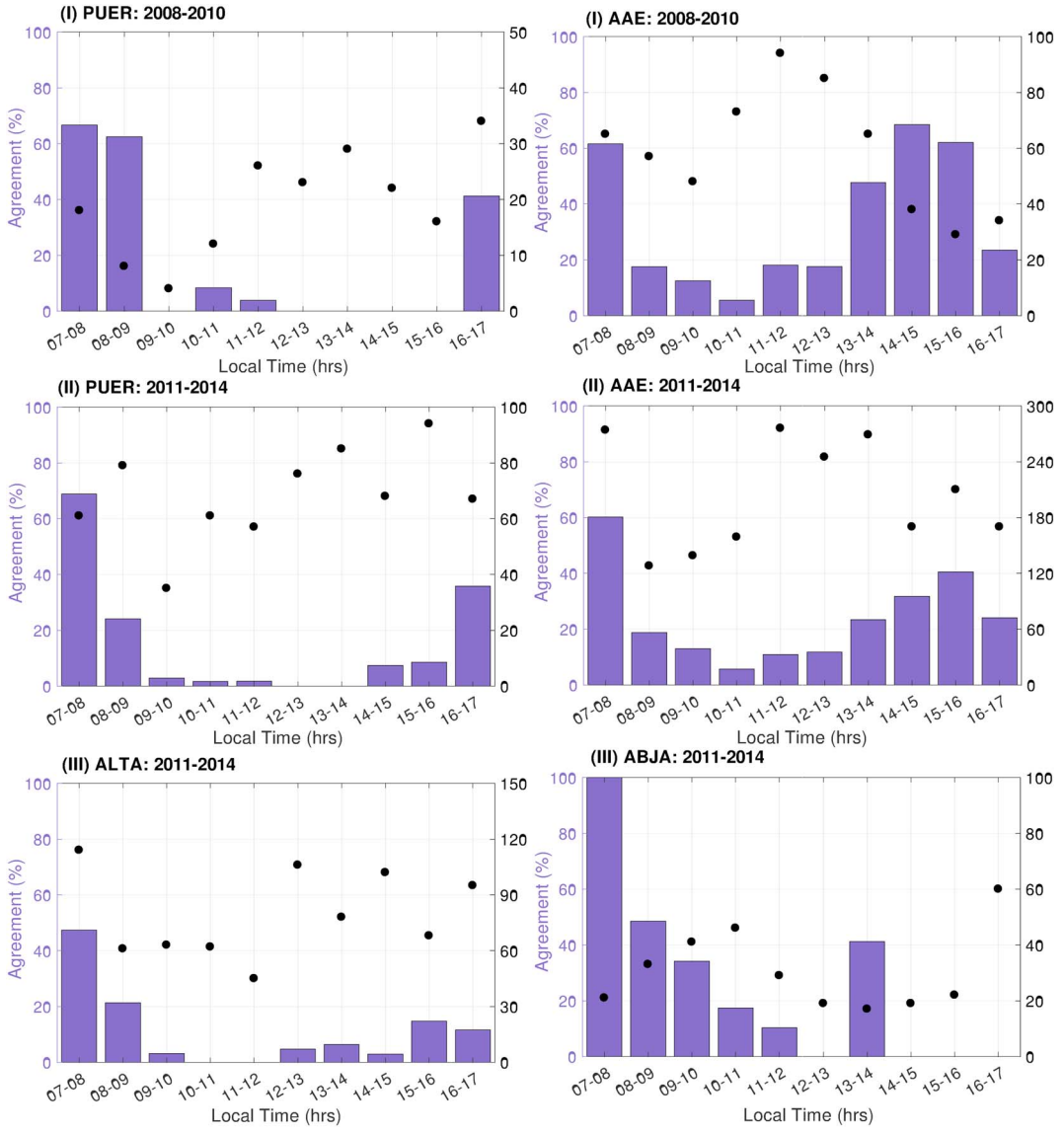

(a) American sector (b) African sector

Figure 6. Percentage agreement for Communications and Navigation Outage Forecasting System and ΔH observations in identifying counter electrojets over (a) American sector and (b) African sector, during 2008–2014.

3.2. Local Time Occurrence of CEJ Over the African Sector

Figure 5 is similar to Figure 4, but for (a) AAE (9.0°N, 38.8°E) and (b) ABJA (10.5°N, 7.6°E) in the African sector. Analyses over AAE (Figure 5a) are for CEJ occurrences obtained from C/NOFS and magnetometer ΔH data for 2008–2010 and 2011–2014, respectively, during local daytime (0700–1700 LT). Similar to Figure 4, the right-hand side represents the total number of data points used to compute the percentage CEJ occurrence (left-hand side) during a 1-hr interval.

C/NOFS satellite observations are consistent in identifying higher CEJ occurrences than ground-based magnetometer ΔH data over both AAE and ABJA (when data are available). However, the rate of CEJ occurrence over the African sector is higher than in the American sector as observed from both C/NOFS satellite and magnetometer measurements. As an example, we shall be comparing AAE and PUER results, since they both have information for 2008–2014. Based on this example, it is estimated that CEJ occurrences averaged over all local times were about 30% and 10% higher over AAE (African sector) than PUER (American sector) for C/NOFS satellite and magnetometer observations, respectively. The difference of 10% is even lower than the reported 40% over the Indian sector within a longitudinal difference of 15° based on magnetometer

data (Chandrasekhar et al., 2017). Apart from differences in the local time occurrence of CEJ, there is little or no average statistical difference in CEJ occurrence rate with respect to different solar activity periods (2008–2010 and 2011–2014) for both C/NOFS and ΔH results. Using magnetometer data in 2009, it was reported that the African sector exhibited more CEJ occurrence rate than the American sector (Rabiu et al., 2017), and this also reflected in the CEJ seasonal dependence analysis as we shall show later. This appears to be the case for an extended period of time given that we have performed a statistical analysis for at least 6 years. Over AAE, both data sets show high frequency of CEJ occurrence rate during the morning and afternoon/evening hours, a result similar to South American sector results with respect to local time trends of CEJ occurrence. Once again, C/NOFS satellite observations largely exhibit more CEJ occurrences than magnetometer data. Concerning earlier satellite CEJ studies, Cohen and Achache (1990) used Magnetic Field Satellite data (average altitude of 400 km) and reported dominant CEJ in morning hours compared to dusk hours but added a caveat about the procedure applied that could have influenced the interpretation of results. Over both African and American sectors, the cases where CEJ events are not captured in magnetometer data may not necessarily mean that they are absent and should be understood within the framework of having limited both magnetometer and C/NOFS satellite data simultaneously available, and yet the latter may be limited due to its orbit period. However, fewer CEJ occurrences during some daytime hours (0900–1100 LT) have previously been reported in the Indian and African sectors (Alex & Mukherjee, 2001) and attributed to increased eastward electric and high gradients in ionospheric conductivity during these local times. Here, we reemphasize that there is more CEJ occurrence rate from magnetometer data in the African sector compared to the American sector. This could be linked to the the longitudinal differences where the magnitude of vertical drift velocity that has been shown to be stronger in the American sector (Yizengaw et al., 2012).

3.3. Agreement of C/NOFS and ΔH Observations in CEJ Identification

Figure 6 demostrates the percentage agreement between C/NOFS satellite and ΔH data in CEJ identification for (a) American sector (PUER [panels I and II] and ALTA [panel III]), and (b) African sector represented by AAE (panels I and II) and ABJA (panel III). In all subplots/panels, the total number of data points within each hour range is plotted (on the right-hand side y axis) as black dots. In Figure 6, the agreement for the two data sets is presented separately during the periods of 2008–2010 and 2011–2014. Although the data set may not be identical because of the amount of data for each individual longitude sector, we observe that the CEJ occurrence rate is different between the African and American sectors, even within each sector itself. It has been reported that the CEJ occurrence may be localized even for smaller longitude separation of about 1 hr (Chandrasekhar et al., 2017), owing to different changes in neutral winds and local electrodynamics (Alex & Mukherjee, 2001; Rangarajan & Rastogi, 1993, and references therein). To a large extent, the diurnal variability of the percentage agreement between C/NOFS satellite and ΔH data in identifying CEJ events follows very closely a similar trend of the CEJ occurrence rate as detected by magnetometer ΔH data. This is clearly visible when comparing ΔH plots in Figures 4 and 5 with Figures 6a and 6b for the American and African sectors, respectively. This implies that most of the CEJ events observed in ΔH data were also captured by the C/NOFS satellite. Up to date, causes of CEJ continue to be a major research subject since their identification by Gouin (1962). Figure 6 also shows that CEJ occurrences are dominant in morning and evening hours, and this has been documented by several experimental and theoretical studies in different longitude sectors (e.g., Alex & Mukherjee, 2001; Chandrasekhar et al., 2017; Hanuise et al., 1983; Marriott et al., 1979; Rabiu et al., 2017, and references therein). It has been demonstrated that contribution of semidiurnal tides exhibiting modes of different magnitudes to the electric field plays a role in the occurrence of CEJs in morning and evening local times over the equator (e.g., Alex & Mukherjee, 2001; Hanuise et al., 1983; Marriott et al., 1979). Stening et al. (1996) argued that CEJ events (termed as reverse electrojet in their paper) are possibly caused by global tidal dynamics with linkage to stratospheric warming. These authors showed that high latitude changes in mean zonal winds within the altitudes 90–100 km were associated with stratospheric warming which will later influence the circulation of global tides thereby contributing to driving of CEJ events. This interpretation was mainly plausible for CEJ events which occurred in northern (southern) winter (summer) hemispheres. Raghavarao and Anandarao (1980) showed that the upliftment of ions by vertical upward winds of sufficient magnitudes (e.g., 13 m/s) can lead to the cancellation and/or reversing of the upward polarization electric field that gives rise to eastward electric field during local daytime. The origin of these vertical winds could be gravity waves that have been shown to have a significant effect in modifying the electrojet within altitudes of 110–150 km (Anandarao, 1976). It is established that the solar terminator contributes to launching of atmospheric gravity waves (e.g., Beer, 1978; Forbes et al., 2008).

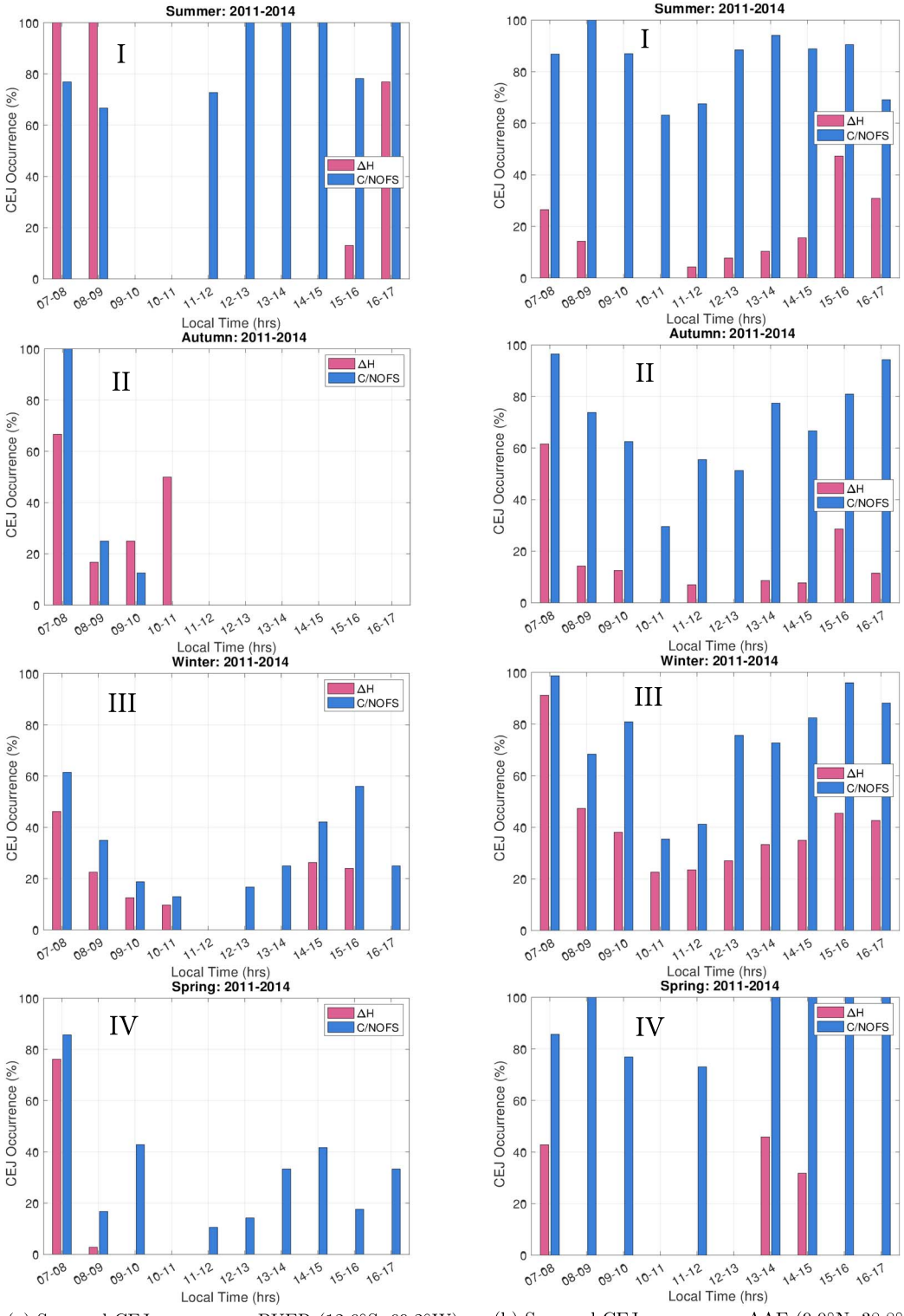

(a) Seasonal CEJ occurrence: PUER (12.6°S, 69.2°W) (b) Seasonal CEJ occurrence: AAE (9.0°N, 38.8°E)

Figure 7. Seasonal occurrence of CEJ (expressed as a percentage) as observed by C/NOFS satellite (blue) and ground-based magnetometers (dark pink) over the American and African sectors during 2011–2014. CEJ = counter electrojet; C/NOFS = Communications and Navigation Outage Forecasting System.

There are therefore a number of suggested dynamic and electrodynamical processes that could contribute to CEJ occurrences, and it is not feasible to point out the dominant mechanism(s) in a statistical study of this nature. Our main emphasis was to establish the agreement/disagreement between C/NOFS satellite and magnetometer data in observing these CEJ occurrences which would later be useful in deciding to combine these data sets for modelling purposes especially that satellite data are attractive for longitudinal observations.

4. Seasonal Dependence of CEJ

For American and African sectors, both C/NOFS satellite vertical ion plasma drift and ΔH observations from 2011 to 2014 (which had substantial amount of data) were categorized according to seasons representing summer (December, January, February), autumn (March–May), winter (June–August) and spring (September–November). The seasonal analysis was limited to 2011–2014 due to substantial missing ΔH data over PUER prior to 2011 to avoid potential cases of generating "statistically biased" results. Figure 3 shows that PUER had fewer number of data points (650) compared to AAE (2,037), and a detailed difference during 2008–2010 can be seen in the first two panels of Figures 4a and 5a for both sectors. Figure 7 shows the percentage seasonal occurrence of CEJ for (a) PUER (12.6°S, 69.2°W), and (b) AAE (9.0°N, 38.8°E) representing the American and African sectors, respectively. The red and blue bars represent CEJ occurrence observed from ΔH and C/NOFS satellite data, respectively.

In all seasons, there are more CEJ events recorded by C/NOFS satellite compared to magnetometer observations. The CEJ occurrence rate is present up to 60% (for C/NOFS satellite data) in the American sector and at all local daytimes in the African sector as revealed by C/NOFS satellite and magnetometer measurements during the winter season. There are times when C/NOFS satellite data only show CEJ events with no single CEJ occurrence detected in magnetometer ΔH data for most of the season. This is more prominent in the American sector especially in summer between 1100 and 1500 LT (Figure 7a, panel I) and spring from 1100 to 1700 LT (see panel IV, Figure 7a). C/NOFS satellite observations show the CEJ occurrence rate in both sectors at all times (except at 1100–1200 LT over the American sector) with more events over the African sector in winter. CEJ occurrence during the Northern Hemisphere winter season has been previously linked to sudden stratospheric warming (Stening et al., 1996). In Figures 7a and 7b, panel I, there is a significant occurrence of CEJs for both American and African sectors especially for C/NOFS satellite observations. C/NOFS satellite observes CEJ occurrence of more than 60% in both African and American sectors, at almost all times (apart from 0900–1100 LT in the American sector). Broadly speaking, CEJ occurrences are more prominent in the African sector than the American sector during all seasons, a result that agrees well with previous studies such as the one of Rabiu et al. (2017) which analyzed geomagnetic data over Huancayo (75.22°W, 12.07°S) and AAE in 2009. Rabiu et al. (2017) showed that CEJ events were consistently present at all seasons over the African sector. In fact, their monthly statistics based on magnetometer data showed that morning CEJs were a common feature up to 100% over AAE apart from months of June, November and December in 2009. Seasonally, we have shown that higher differences in CEJ occurrence rate between the African and American sectors for both C/NOFS satellite and magnetometer observations is in the Southern Hemisphere winter (June–August), a finding similar to results reported in Soares et al. (2018), and attributed to the dominance of wave-4 pattern. This is also consistent with the most recent comprehensive climatological analysis based on CHAMP satellite data which showed that CEJ occurrence rate peaks around July–August (Zhou et al., 2018). Previous seasonal analyses of vertical $\mathbf{E} \times \mathbf{B}$ drift in different longitude sectors revealed that the C/NOFS satellite observes more downward drifts or negative $\mathbf{E} \times \mathbf{B}$ drift values (corresponding to CEJ in this study) in the African sector than the American sector (Yizengaw & Groves, 2018; Yizengaw et al., 2014). These authors further showed that December and June solstices exhibit largely negative C/NOFS vertical $\mathbf{E} \times \mathbf{B}$ drift in the African sector (AAE) which agrees with our winter and summer seasons analyses. For both December and June solstice as well as March/September equinox months, Yizengaw and Groves (2018) reported average upward/positive vertical $\mathbf{E} \times \mathbf{B}$ drift variability from C/NOFS satellite observations. Conditions favorable for CEJ occurrence would have to involve generation of reverse current with magnitudes greater than the background eastward electric field over the equator. It is remarked that locations with strong EEJ record the lowest CEJ occurrence rate as is the case with this study. It is known that the American sector exhibits strong EEJ strength (e.g., Rabiu et al., 2017; Yizengaw et al., 2014) compared to the African sector. To understand the relative contribution of different physical processes such as upward vertical winds possibly related to gravity waves (Raghavarao & Anandarao, 1980) and tidal effects

(Stening et al., 1996), extensive neutral wind data are necessary in both sectors. This is an issue for further investigations when data become available, especially in the African sector. While other sources make a similar/related observation, it is particularly useful to establish that C/NOFS satellite data are consistent with magnetometer and other ground-based data in identifying the CEJ seasonal dependence. To our knowledge, this is the first study that has shown this statistical confirmation using C/NOFS satellite data moreover in both African and American sectors.

5. Conclusions

We have presented statistical analyses of CEJ occurrences based on ground-based magnetometer and C/NOFS satellite observations over the South American and African regions during 2008–2014. Due to the extended deep solar minimum from 2008–2009, we performed the analysis by considering periods 2008–2010 and 2011–2014 separately. On average, we found no significant difference in CEJ occurrence rate during the extremely low solar activity period of 2008–2010 compared to 2011–2014 in both African and American sectors, an observation that is found for both satellite and magnetometer measurements. However, the frequency of CEJ occurrence was found to be greater in C/NOFS satellite data than magnetometer observations in the African and American sectors. The interpretation of this difference partly lies in the fact that the EEJ/CEJ derived from magnetometer data is a representation of electric current system in the ionospheric E region (90–110 km) which is basically over 300 km below the altitude of the C/NOFS satellite. In general, we have observed that CEJ occurrences are more prevalent in the local morning and afternoon/evening, a result that agrees with existing literature (e.g., Alex & Mukherjee, 2001; Chandrasekhar et al., 2017; Rabiu et al., 2017; Soares et al., 2018; Venkatesh et al., 2015). The C/NOFS satellite data found significant CEJ occurrence in the afternoon hours compared to magnetometer observations over both American and African sectors. For the American sector, a similar observation has been reported while comparing C/NOFS satellite and 150-km echo drifts data from Jicamarca (Rodrigues et al., 2015), which was interpreted to be a result of increased magnitudes of the semidiurnal tides influence in the topside ionosphere (Stoneback et al., 2011). This is the first detailed statistical analysis dedicated to CEJ occurrence as observed by the C/NOFS satellite over the African sector. However, there exist studies that look at general trends of the ionospheric electrodynamics using various data sources including C/NOFS satellite data (Yizengaw et al., 2011, 2014). This study is therefore particularly relevant in interpreting results generated by ionospheric electrodynamics models developed by combining ground-based and satellite observations given that the latter are attractive in regions inaccessible for instrumentation deployment such as over the oceans.

Acknowledgments
Data for the C/NOFS satellite were obtained from the website (http://spdf.gsfc.nasa.gov/pub/data/cnofs/cindi/). The C/NOFS mission is supported by the Air Force Research Laboratory, the Department of Defense Space Test Program, the National Aeronautics and Space Administration (NASA), the Naval Research Laboratory, and the Aerospace Corporation. Magnetometer data were obtained from the AMBER (http://magnetometers.bc.edu/), INTERMAGNET (www.intermagnet.org), and LISN (http://lisn.igp.gob.pe/data/) networks. All these data are freely available. The authors thank the AMBER and SAMBA teams for the magnetometer data. AMBER is operated by Boston College and funded by NASA and AFOSR. Different national institutes which support collected geomagnetic data are acknowledged. Thanks to INTERMAGNET for promoting high standards of magnetic observatory practice. LISN is a project led by the University of Texas at Dallas in collaboration with the Geophysical Institute of Peru and other institutions that provide information in benefit of the scientific community. This work is based on the research supported in part by the National Research Foundation of South Africa (grant 105778); opinions, findings, and conclusions or recommendations expressed in this paper are of the author(s), and the NRF accepts no liability whatsoever in this regard. The work by G. L. and M. B. M. was supported by NSF OISE1459911 and AGS1450512. E. Y.'s work has been partially supported by the Aerospace Corporation SERPA program.

References

Alex, S., & Mukherjee, S. (2001). Local time dependence of the equatorial counter electrojet effect in a narrow longitudinal belt. *Earth, Planets and Space*, *53*, 1151–1161.

Anandarao, B. G. (1976). Effects of gravity wave winds and wind shears on equatorial electrojet. *Geophysical Research Letters*, *3*(9), 545–548.

Anderson, D., Anghel, A., Chau, J., & Veliz, O. (2004). Daytime vertical $E \times B$ drift velocities inferred from ground-based magnetometer observations at low latitudes. *Space Weather*, *2*, S11001. https://doi.org/10.1029/2004SW000095

Anderson, D., Anghel, A., Yumoto, K., Ishitsuka, M., & Kudeki, E. (2002). Estimating daytime vertical $E \times B$ drift velocities in the equatorial F region using ground-based magnetometer observations. *Geophysical Research Letters*, *29*(12), 1596. https://doi.org/10.1029/2001GL014562

Beer, T. (1978). On atmospheric wave generation by the terminator. *Planetary and Space Science*, *26*(2), 185–188.

Chandrasekhar, N. P., Archana, R. K., Nagarajan, N., & Arora, K. (2017). Variability of equatorial counter electrojet signatures in the Indian region. *Journal of Geophysical Research: Space Physics*, *122*, 2185–2201. https://doi.org/10.1002/2016JA022904

Chen, Y., Liu, L., & Wan, W. (2011). Does the $F_{10.7}$ index correctly describe solar EUV flux during the deep solar minimum of 2007–2009? *Journal of Geophysical Research*, *116*, A04304. https://doi.org/10.1029/2010JA016301

Cohen, Y., & Achache, J. (1990). New global vector magnetic anomaly maps derived from MAGSAT data. *Journal of Geophysical Research*, *95*(B7), 10,783–10,800.

Dubazane, M. B, & Habarulema, J. B. (2018). An empirical model of vertical plasma drift over the African sector. *Space Weather*, *16*, 619–635. https://doi.org/10.1029/2018SW001820

Ezquer, R. G., López, J. L., Scidá, L. A., Cabrera, M. A., Zolesi, B., Bianchi, C., et al. (2014). Behaviour of ionospheric magnitudes of F_2 region over Tucumán during a deep solar minimum and comparison with the IRI 2012 model predictions. *Journal of Atmospheric and Solar-Terrestrial Physics*, *107*, 89–98. https://doi.org/10.1016/j.jastp.2013.11.010

Fambitakoye, O., Mayaud, P. N., & Richmond, A. D. (1976). Equatorial electrojet and regular daily variation S_R - III. Comparison of observations with a physical model. *Journal of Atmospheric and Terrestrial Physics*, *38*(2), 113–121. https://doi.org/10.1016/0021-9169(76)90118-5

Fang, T. W., Richmond, A. D., Liu, J. Y., & Maute, A. (2008). Wind dynamo effects on ground magnetic perturbations and vertical drifts. *Journal of Geophysical Research*, *113*, A11313. https://doi.org/10.1029/2008JA013513

Fejer, B. G., Jensen, J. W., & Su, S.-Y. (2008). Quiet time equatorial F region vertical plasma drift model derived from ROCSAT-1 observations. *Journal of Geophysical Research*, *113*, A05304. https://doi.org/10.1029/2007JA012801

Fejer, B. G., & Scherliess, L. (1998). Mid- and low-latitude prompt ionospheric zonal plasma drifts. *Geophysical Research Letters*, *25*(16), 3071–3074.

Forbes, J. M., Bruinsma, S. L., Miyoshi, Y., & Fujiwara, H. (2008). A solar terminator wave in thermosphere neutral densities measured by the CHAMP satellite. *Geophysical Research Letters*, *35*, L14802. https://doi.org/10.1029/2008GL034075

Gouin, G. (1962). Reversal of the magnetic daily variation at Addis Ababa. *Nature*, *193*, 1145–1146.

Gustafsson, G., Papitashvili, N. E., & Papitashvili, V. O. (1992). A revised corrected geomagnetic coordinate system for epochs 1985 and 1990. *Journal of Atmospheric and Terrestrial Physics*, *54*, 1609–1631.

Habarulema, J. B., Dubazane, M. B., Katamzi-Joseph, Z. T., Yizengaw, E., Moldwin, M. B., & Uwamahoro, J. C. (2018). Long-term estimation of diurnal vertical E×B drift velocities using C/NOFS and ground-based magnetometer observations. *Journal of Geophysical Research: Space Physics*, 6996–7010. https://doi.org/10.1029/2018JA025685

Hanuise, C., Mazaudier, C., Vila, P., Blanc, M., & Crochet, M. (1983). Global dynamo simulation of ionospheric currents and their connection with the equatorial electrojet and counter-electrojet: A case study. *Journal of Geophysical Research*, *88*(A1), 253–270.

Huber, P. J (1981). *Robust statistics*. New York: John Wiley.

Huber, P. J, & Ronchetti, E. M. (2009). *Robust statistics: Second edition*. New York: John Wiley.

Kikuchi, T., Lühr, H., Schlegel, K., Tachihara, H., Shinohara, M., & Kitamura, T.-I. (2000). Penetration of auroral electric fields to the equator during a substorm. *Journal of Geophysical Research*, *105*(A10), 23,251–23,261.

Kumar, S., Veenadhari, B., Tulasi Ram, S., Su, S.-Y., & Kikuchi, T. (2016). Possible relationship between the equatorial electrojet (EEJ) and daytime vertical $E \times B$ drift velocities in F region from ROCSAT observations. *Advances in Space Research*, *58*, 1168–1176. https://doi.org/10.1016/j.asr.2016.06.009

Lomidze, L., Knudsen, D. J., Burchill, J., Kouznetsov, A., & Buchert, S. C. (2017). Calibration and validation of swarm plasma densities and electron temperatures using ground-based radars and satellite radio-occultation measurements. *Radio Science*, *53*, 15–36. https://doi.org/10.1002/2017RS006415

Lühr, H., Maus, S., & Rother, M. (2004). Noon-time equatorial electrojet: Its spatial features as determined by the CHAMP satellite. *Journal of Geophysical Research*, *109*, A01306. https://doi.org/10.1029/2002JA009656

Marriott, R. T., Richmond, A. D., & Venkateswaran, S. V. (1979). The quiet-time equatorial electrojet and counter-electrojet. *Journal of Geomagnetism and Geoelectricity*, *31*, 311–340.

Mayaud, P. N. (1977). The equatorial counter-electrojet—A review of its geomagnetic aspects. *Journal of Atmospheric and Terrestrial Physics*, *39*(9-10), 1055–1070. https://doi.org/10.1016/0021-9169(77)90014-9

Patra, A. K., Chaitanya, P. P., Otsuka, Y., Yokoyama, T., Yamamoto, M., Stoneback, R. A., & Heelis, R. A. (2014). Vertical $\mathbf{E} \times \mathbf{B}$ drifts from radar and C/NOFS observations in the Indian and Indonesian sectors: Consistency of observations and model. *Journal of Geophysical Research: Space Physics*, *119*, 3777–3788. https://doi.org/10.1002/2013JA019732

Patra, A. K., Yokoyama, T., Otsuka, Y., & Yamamoto, M. (2008). Daytime 150 km echoes observed with the Equatorial Atmosphere Radar in Indonesia: First results. *Geophysical Research Letters*, *119*, L06101. https://doi.org/10.1029/2007GL033130

Rabiu, A. B., Folarin, O. O., Uozumi, T., Hamid, N. S. A., & Yoshikawa, A. (2017). Longitudinal variation of equatorial electrojet and the occurrence of its counter electrojet. *Annales Geophysicae*, *35*, 535–545. https://doi.org/10.5194/angeo-35-535-2017

Raghavarao, R., & Anandarao, B. G. (1980). Vertical winds as a plausible cause for equatorial counter electrojet. *Geophysical Research Letters*, *7*(5), 357–360.

Rangarajan, G. K., & Rastogi, R. G. (1993). Longitudinal difference in magnetic field variations associated with quiet day counter electrojet. *Journal of Geomagnetism and Geoelectricity*, *45*(8), 649–656.

Rastogi, R. G. (1974a). Westward equatorial electrojet during daytime hours. *Journal of Geophysical Research*, *79*(10), 1503–1512.

Rastogi, R. G. (1974b). Lunar effects in the counter electrojet near the magnetic equator. *Journal of Atmospheric and Terrestrial Physics*, *36*(1), 167–170. https://doi.org/10.1016/0021-9169(74)90074-9

Rodrigues, F. S., Smith, J. M., Milla, M., & Stoneback, R. A. (2015). Daytime ionospheric equatorial vertical drifts during the 2008–2009 extreme solar minimum. *Journal of Geophysical Research: Space Physics*, *120*, 1452–1459. https://doi.org/10.1002/2014JA020478

Siddiqui, T. A., Maute, A., Pedatella, N., Yamazaki, Y., Lühr, H., & Stolle, C. (2018). On the variability of the semidiurnal solar and lunar tides of the equatorial electrojet during sudden stratospheric warmings. *Annales Geophysicae*, *36*, 1545–1562.

Singh, D., Gurubaran, S., & He, M. (2018). Evidence for the influence of DE3 tide on the occurrence of equatorial counterelectrojet. *Geophysical Research Letters*, *45*, 2145–2150. https://doi.org/10.1002/2018GL077076

Soares, G., Yamazaki, Y., Matzka, J., Pinheiro, K., Morschhauser, A., Stolle, A., & Alken, P. (2018). Equatorial counter electrojet longitudinal and seasonal variability in the American sector. *Journal of Geophysical Research: Space Physics*, *123*, 9906–9920. https://doi.org/10.1029/2018JA025968

Stening, R. J., Meek, C. E., & Manson, A. H. (1996). Upper atmosphere wind systems during reverse equatorial electrojet events. *Geophysical Research Letters*, *23*(22), 3243–3246.

Stolle, C., Manoj, C., Lühr, H., Maus, S., & Alken, P. (2008). Estimating the daytime equatorial ionization anomaly strength from electric field proxies. *Journal of Geophysical Research*, *113*, A09310. https://doi.org/10.1029/2007JA012781

Stoneback, R. A., Davidson, R. L., & Heelis, R. L. (2012). Ion drift meter calibration and photoemission correction for the C/NOFS satellite. *Journal of Geophysical Research*, *117*, A08323. https://doi.org/10.1029/2012JA017636

Stoneback, R., Heelis, R., Burrell, A., Coley, W., Fejer, B. G., & Pacheco, E. (2011). Observations of quiet time vertical ion drift in the equatorial ionosphere during the solar minimum period of 2009. *Journal of Geophysical Research*, *116*, A12327. https://doi.org/10.1029/2011JA016712

Valladares, C. E., & Chau, J. L. (2012). The Low-Latitude Ionosphere Sensor Network: Initial results. *Radio Science*, *47*, RS0L17. https://doi.org/10.1029/2011RS004978

Venkatesh, K., Fagundes, P. R., Prasad, D. S. V. V. D., Denardini, C. M., de Abreu, A. J., de Jesus, R., & Gende, M. (2015). Day-to-day variability of equatorial electrojet and its role on the day-to-day characteristics of the equatorial ionization anomaly over the Indian and Brazilian sectors. *Journal of Geophysical Research: Space Physics*, *120*, 9117–9131. https://doi.org/10.1002/2015JA021307

Vineeth, C., Pant, T. K., & Sridharan, R. (2009). Equatorial counter electrojets and polar stratospheric sudden warmings—A classical example of high latitude-low latitude coupling? *Annales de Geophysique*, *27*, 3147–3153.

Yizengaw, E., & Groves, K. M. (2018). Longitudinal and seasonal variability of equatorial ionospheric irregularities and electrodynamics. *Space Weather*, *16*, 946–968. https://doi.org/10.1029/2018SW001980

Yizengaw, E., & Moldwin, M. B. (2009). African Meridian B-field Education and Research (AMBER) array. *Earth, Moon, and Planets*, *104*, 237–246. https://doi.org/10.1007/s11038-008-9287-2

Yizengaw, E., Moldwin, M. B., Mebrahtu, A., Damtie, B., Zesta, E., Valladares, C. E., & Doherty, P. H. (2011). Comparison of storm time equatorial ionospheric electrodynamics in the African and American sectors. *Journal of Atmospheric and Solar-Terrestrial Physics*, *73*(1), 156–163.

Yizengaw, E., Moldwin, M. B., Zesta, E., Biouele, C. M., Damtie, B., Mebrahtu, A., et al. (2014). The longitudinal variability of equatorial electrojet and vertical drift velocity in the African and American sectors. *Annales Geophysicae*, *32*, 231–238.

Yizengaw, E., Zesta, E., Moldwin, M. B., Damtie, B., Mebrahtu, A., Valladares, C. E., & Pfaff, R. F. (2012). Longitudinal differences of ionospheric vertical density distribution and equatorial electrodynamics. *Journal of Geophysical Research*, *117*, A07312. https://doi.org/10.1029/2011JA017454

Zhou, Y.-L., Lühr, H., Xu, H.-W., & Alken, P. (2018). Comprehensive analysis of the counter equatorial electrojet: Average properties as deduced from CHAMP observations. *Journal of Geophysical Research: Space Physics*, *123*, 5159–5181. https://doi.org/10.1029/2018JA025526